

ROISegNet: A Deep Learning Framework for Automatic Segmentation of Region of Interest from Breast Thermogram Imagery

¹Preethi Veerlapalli ²Dr. Kakali Das,

Submitted: 25/01/2024 Revised: 03/03/2024 Accepted: 11/03/2024

Abstract: Among the top causes of mortality for women worldwide is breast cancer. With the emergence of non-invasive imaging technology known as breast thermography, it is possible to know abnormalities in breast that may lead to breast cancer over a period of time. Therefore, early detection of breast cancer probability could save lives and get rid of such cancer altogether. At the same time, Artificial Intelligence (AI) has become a technology innovation for solving problems in healthcare domain. In this context, it is indispensable to exploit AI enabled methods such as deep learning and breast thermography for early detection of breast cancer. However, the research in this paper is confined to breast Region of Interest (ROI) segmentation using deep learning to facilitate mechanisms for breast cancer screening later. Existing deep learning model named atrous convolution is found suitable for semantic segmentation. Our deep learning system, ROISegNet, was suggested for automated segmentation of ROI from breast thermogram imagery. Our framework uses atrous convolution as part of encoder and designs decoder module for leveraging efficiency in semantic segmentation. We proposed an algorithm named Learning based Breast ROI Segmentation (LbBROIS) to realize our framework. Our empirical study made with the benchmark dataset DMR-IR revealed with, ROISegNet outperforms existing models such as VGG19, ResNet50, InceptionV3 and Atrous Convolution with highest accuracy 98.63%.

Keywords: Deep Learning, Region of Interest Segmentation, Breast Cancer, Atrous Convolution, Sematic Image Segmentation

1. Introduction

Among women worldwide, one of the most common malignancies to receive a diagnosis is breast cancer [1]. In women, breast cancer accounted for more than 15% of all cases of cancer-related deaths of late [2]. Imaging methods, medical professionals, and self-examination are all useful in identifying breast problems. The only way to determine if cancer is present or absent is by a biopsy [4]. Many breast imaging modalities, including ultrasound and mammography, are currently being used to detect breast cancer early. The most used screening method is mammography due to its high detectability, affordability, and passably accurate results. Mammograms are a very accurate imaging technique that may be used to identify and classify breast cancer. Nonetheless, there are few instances when it is known to work poorly, particularly in individuals with thick breast tissue. In addition, young women may experience severe ionizing radiation adverse effects. Furthermore, mammography is known to have difficulty picking up tiny lesions smaller than 2 mm. Because of these drawbacks, thermography—a newly developed method for screening for breast cancer—is much sought after. A low-cost, non-invasive, non-inclusive, radiation-free method is thermography [2].

Thus, it can be used to detect breast cancer in its early stages in young women and those with large breasts. Since all biological things release infrared (IR) radiation above absolute zero, this is the central hypothesis of thermography. For the purposes of breast thermography, an infrared thermal camera transforms infrared radiation into electrical impulses that are shown as a thermogram. Its unique temperature scale highlights potential abnormalities and makes them stand out from normal tissue [17]. Compared to mammography, breast thermography has a number of benefits, such as its comfort for male patients, its efficacy in all age groups, and its capacity to operate with thick breast tissue. Breast cancer can be detected early because to thermography's reputation for being rapid, safe and accurate. Breast area segmentation is an essential step in any breast cancer detection system. It is a method of separating the breast region from other body areas in thermal images [16]. The excised region must contain, as much as possible, all breast tissues, ducts, lobules, and lymph nodes. The procedure of segmenting breasts can be done entirely manually or entirely automatically. Most scientific research opts to use a manual or semi-automated method to remove the breast area extraction procedure due to the amorphous nature of each breast and the absence of distinct borders in these kinds of pictures. Scientific studies over the past few decades have concentrated on machine learning techniques related to thermography-based breast cancer diagnosis; some researchers have focused on identifying the size and location of tumors, but

¹Department of Computer Science and Engineering, Koneru Lakshmaiah Education Foundation, Hyderabad-500075, Telangana, India.

²Department of Computer Science and Engineering, Koneru Lakshmaiah Education Foundation, Hyderabad-500075, Telangana, India.

Emails: ¹preethireddyveerlapalli@gmail.com

²kakali.das@klh.edu.in

other researchers have focused on characteristics such as breast quadrants and collection techniques. Deep learning is one machine learning method that uses multilayer convolutional neural networks (CNN). Features may be automatically extracted from a training dataset via deep learning [18]. Researchers have used CNNs to diagnose breast cancer with encouraging results in recent years. In the past, CNNs were not frequently used for the thermal imaging-based breast cancer detection process because of their inferior efficiency when compared to textural or statistical features, or maybe because of their high computational weight [3]. In recent years, CNNs were thought to be among the best methods for pattern recognition. During the training process of CNN models, the thermal picture includes unnecessary regions such as the neck, shoulder, chest, and other body parts that act as noise. The poor spatial resolution of thermography pictures makes them challenging to interpret. As a result, extracting the breast region from the thermal images is essential since the segmentation findings have a significant impact on the classification process's outcome. Breast cancer, as was previously said, is considered to be one of the leading causes of death for women. Therefore, early detection is crucial to save lives. Thermography imaging, which uses infrared technology, is an effective diagnostic technique for the detection of breast cancer; however, the radiologist's interpretation of the thermogram determines the thermogram's usefulness. To the best of our knowledge, the earlier work has several shortcomings. These comprise: (1) limitations related to the dataset; (2) researches of related work that segmented the breast area manually or without consideration before classification; (3) segmentation models that eliminated parts of the breast; and (4) researches that assessed their model solely based on the accuracy metric. But, in the event that the dataset is unbalanced, a high accuracy rate does not guarantee that the model can distinguish between all classes equally. Our paper is limited to the segmentation of the breast area using thermal images. Little research has been done on breast ROI segmentation using deep learning with encoder-decoder architecture, according to the literature survey. Here are the things we have contributed.

1. We proposed a deep learning framework known as ROIsegNet for automatic segmentation of ROI from breast thermogram imagery. Our framework uses atrous convolution as part of encoder and designs decoder module for leveraging efficiency in semantic segmentation.
2. We proposed an algorithm named Learning based Breast ROI Segmentation (LbBROIS) to put our framework into practice.

3. We developed a program to assess ROIsegNet. Our empirical study made with the benchmark dataset DMR-IR revealed that, ROIsegNet outperforms existing models such as VGG19, ResNet50, InceptionV3 and Atrous Convolution.

This is how the rest of the paper is organized. In Section 2, previous research on semantic picture segmentation in thermal images of breasts is reviewed. Our methodology and underlying structure are presented in Section 3. Section 4 reports on our empirical study's findings. Section 5 not only outlines certain limitations but also explores the relevance of our technique. Our task is concluded in Section 6.

2. Related Work

This section reviews prior works on thermal image based breast segmentation towards breast cancer diagnosis. Karthiga and Narasimhan [1] explored a new thermography technique that uses machine learning and infrared images to identify breast cancer. Cubic SVM yields accuracy rate with improved ROI selection, morphological procedures, and curvelet transform. Yadav and Jadhav [2] used radiation-free thermal infrared imaging that helps in early illness detection by Thermography. Thermal scan analysis by machine learning offers more efficient non-invasive medical diagnostic options than mammography. Cauce *et al.* [3] suggested a novel approach to identifying breast cancer uses a multi-input CNN to blend personal/clinical data with thermal imaging, greatly increasing diagnosis accuracy. Macedo *et al.* [4] diagnosed breast cancer is critical, and mammography is painful even when it works well. Accuracy in breast thermography is increased with machine learning support. Abhisheka *et al.* [5] observed that with more than 2.1 million diagnoses each year, (BC) is a global challenge. Improved survival rates depend heavily on early diagnosis, which is made possible by AI-based methods. The study intends to direct future research toward the creation of automated, dependable BC diagnosis models.

Tsietso *et al.* [6] opined that an important global problem is breast cancer, which highlights the need of early detection. With the combination of clinical data and several perspectives of breast thermograms, this study presents a multi-input CADx system. Improved sensitivity in the results point to a potentially safer and less expensive screening method. Rajinikanth *et al.* [7] found that it is critical to diagnose breast cancer early. With the use of breast thermal images, this work creates an automated detection method that uses a Decision-Tree classifier to achieve over accuracy. Houssein *et al.* [8] stated that being the primary cause of mortality for women, breast cancer necessitates precise early identification. With a focus on trends and problems, this paper examines machine and

deep learning applications in multi-modal medical imaging. Mashekova *et al.* [9] affected people of both genders and requires early detection with BC. Improved technology has led to a rise in interest in thermography despite its limits. Although it needs more research and development, artificial intelligence improves accuracy. Resmini *et al.* [10] highlighted how important early detection is. A non-invasive technique that shows promise for screening and diagnosis is thermography. The presented technique shows promise, and further developments are recommended.

Houssein *et al.* [11] helped to identify aberrant temperature variations that may be indicative of breast cancer. An improved chimp optimization algorithm (IChOA) outperforms competitors in terms of performance metrics and accuracy when it comes to picture segmentation. Larger datasets and machine learning hybridization are the goals of future study. Lakshman *et al.* [12] highlighted the increasing number of instances of carcinoma and highlights its high death rate and severity. When it comes to carcinoma detection, Random Forest performs better than Support Vector Machine, with a higher accuracy rate. Zeiser *et al.* [13] accreted diagnosis of breast cancer is aided by the CNN model DeepBatch, which improves WSI segmentation. With promise for other malignancies, it improves cellular interpretation. Pre-training of ResNet-50, multimodal exploration, detection of micrometastases, and ethical issues are the future objectives. Rezaei *et al.* [14] improved survival rates from breast cancer, a worldwide hazard to women, depend on early identification. With an emphasis on 2016–2020, this research examines image-based diagnostic techniques. Complexity, expense, reliance on humans, and accuracy are challenges. Future paths prioritize tackling large data difficulties, taking patient information into account, and merging modalities. Liu *et al.* [15] achieved higher accuracy than previous approaches by putting out a deformable attention VGG19 model for automatic metastasis prediction of axillary lymph nodes in breast cancer CECT images. Through daily diagnostic support, the algorithm lessens the effort for clinicians. Three-dimensional analysis, enhanced lesion detection, and multi-center validation are the goals of future research.

Krithiga and Geetha [16] issued with sensitivity and specificity are highlighted while comparing the prediction of breast cancer recurrence using deep learning and machine learning. With an emphasis on accuracy gains and possible big data analytics applications, the paper evaluates several features and approaches for histopathology image interpretation. Sharma *et al.* [17] approached utilizing shearlet transform and superpixel-based ROI segmentation is suggested for the identification of anomalies in breast thermograms. Reaches a high

degree of classification precision and resilience against false coloration. Bai *et al.* [18] used by deep learning in breast cancer screening, particularly in conjunction with digital breast tomosynthesis (DBT), transforms diagnostic imaging and ensures technological flexibility. Yousefi *et al.* [19] addressed the difficulties in basis selection and presents Deep-SemiNMF for breast cancer thermography. With an accuracy rate of 71.36%, the model has notable categorization capability. Chen *et al.* [20] combined the subject expertise of radiologists to provide a breast cancer CEUS video classification model that achieves 86.3% accuracy sensitivity.

Tariq *et al.* [21] innovated in medical imaging improve early detection of breast cancer. Effective computer-aided detection is made possible by AI and computer vision, which categorize anomalies from imaging modalities. Bakx *et al.* [22] evaluated a deep learning model to segment breast cancer radiation, guaranteeing both qualitative and quantitative analysis for therapeutic use. Yadav *et al.* [23] investigated the use of deep learning, machine learning, and hybrid techniques for breast cancer diagnosis using Wisconsin databases and mammography datasets. Among classifiers, SVM has the best accuracy. Dimension reduction and ensemble machine learning approaches may be used in future studies. Li and Lu [24] suggested a model that uses U-Net for segmentation and ResNet101 or MobileNetV2 for the detection of breast cancer. The competitive results help pathologists identify patients quickly and accurately. Kadry *et al.* [25] created a computer program that uses the Slime Mold Algorithm and Watershed Segmentation to identify breast tumours in MRI slices. Image performance metrics are used to show clinical importance.

Peng *et al.* [26] improved results by applying deep learning radiology to examine patient treatment in advanced breast cancer. Larger datasets and ideal architecture are needed to overcome challenges in ultrasound-based deep learning. Multimodal analysis is advised for future study. Krishna and George [27] suggested a portable infrared imaging system that combines thermography, machine learning, and real-time communication to monitor breast health in isolated areas. Future plans call for improving accessibility, growing the dataset, and adding more perspectives to create a more complete CAD system. Pereira *et al.* [28] suggested by using breast thermography for cancer detection with improved attribute selection. Positive outcomes point to the possibility of increased generality and accuracy. Age limits and a small database size are among the limitations. Plans for the future include growing the dataset and investigating additional characteristics and selection techniques. Meenalochini and kumar [29] highlighted the critical significance mammography plays in the early identification of breast cancer. It examines machine

learning methods with an emphasis on how well they classify data. Similar kind of research was found in [30].

Ibrahim *et al.* [31] explained a technique for segmenting breast cancer from thermal pictures by tweaking quick-shift settings and applying the suggested Chaotic Salp Swarm Algorithm (CSSA). Strong segmentation results for breast cancer diagnosis are obtained by the CSSA method, which improves convergence and accuracy. Kakileti *et al.* [32] highlighted the value of thermal imaging for early breast cancer diagnosis. To achieve precise, view-independent segmentation, it suggests a cascaded CNN architecture and shows a high dice index. Husaini *et al.* [33] emphasized the importance of breast cancer and the need for early detection techniques. Combining AI with thermography has potential. Review topics are presented together with open research questions. Raghavendra *et al.* [34] developed at critical times and is more common in women by BC. Thermography facilitates analysis. This research reviews how computer-aided diagnosis improves accuracy. Farooq and Corcoran [35] enhanced by human thermography, an essential medical instrument. COVID-19 and cancer detection are made easier with the use of infrared thermography. In classifying breast tumours, the proposed CNN method achieves 80% accuracy.

Singh *et al.* [36] explored on early identification of breast cancer probability. Together with mammography, infrared breast thermography facilitates painless, non-invasive diagnostics. Reliability is improved by machine learning. Kakileti *et al.* [37] addressed breast cancer, a major cause of death that is particularly prevalent in underdeveloped countries due to delayed identification. The study lays the groundwork for validation on a larger and more varied population in the future. Ruiz *et al.* [38] suggested an automatic technique that uses statistical characteristics to achieve competitive for the categorization of breast thermography images. Future research aims to extract all textural characteristics from GLCM and explore the use of CNN—a type of deep learning—as a feature extractor. Mahmood *et al.* [39] highlighted the difficulties in diagnosing breast cancer because of misunderstandings and calls for effective deep learning-based techniques. The study evaluates segmentation, classification, and modality and suggests enhancements for consistent results. Gomathi *et al.* [40] presented Adaptive Median Filter and Unsupervised Anisotropic-Feature Transformation as a means of automating breast cancer diagnosis. Prospective outcomes in identifying variants impacted by cancer and the

possibility of identifying breast cancer are demonstrated by the suggested method, which stimulates more investigations. As may be seen from the literature review, there is little research on breast ROI segmentation using deep learning with encoder-decoder architecture.

3. Proposed Framework

Our deep learning framework was suggested known as ROISegNet for automatic division of ROI from breast thermograms. The framework is based on the design of encoder-decoder made up of atrous convolution as part of encoder and a customized decoder network. The given input breast thermal image is subjected to efficient segmentation to obtain ROI (breast region) which helps in automatic detection of abnormalities that might lead to breast cancer in future. In other words, working with thermograms has potential to detect probability of breast cancer early. In this context, the proposed deep learning framework ROISegNet, shown in Figure 1, assumes significance. The process of extracting dense features for semantic segmentation using atrous convolution is an important part of the framework.

3.1 Dense Feature Extraction

Semantic segmentation tasks have shown to be successfully completed by Fully Convolutional Deep Convolutional Neural Nets (DCNNs) [42] when applied [43]. Despite this the spatial resolution of the resultant feature maps is greatly reduced by the repetitive combination of max-pooling and striding at successive layers of these networks, usually by a factor of 32 in each direction in modern DCNNs [44], [45] have used deconvolutional layers to regain the spatial resolution. Alternatively, we suggest utilizing atrous convolution, which was initially developed in [46] for effectively computing the undecimated wavelet transform and was previously used by [47] in the context of DCNN. As per Eq. 1, for two-dimensional signals, an intense convolution is performed at every point i over the output y and a filter w over the input feature map x .

$$y[i] = \sum_k x[i + r.k]w[k] \quad (1)$$

Convolution with up sampled filters, which is known as atrous convolution, and it is produced by inserting $r - 1$ zeros between each subsequent filter value along each spatial dimension. This is the same as sampling the input signal at an r -step pace. By adjusting the rate value via atrous convolution, the filter's field of view may be changed adaptively. Whereas Rate $r = 1$ is a specific instance of conventional convolution.

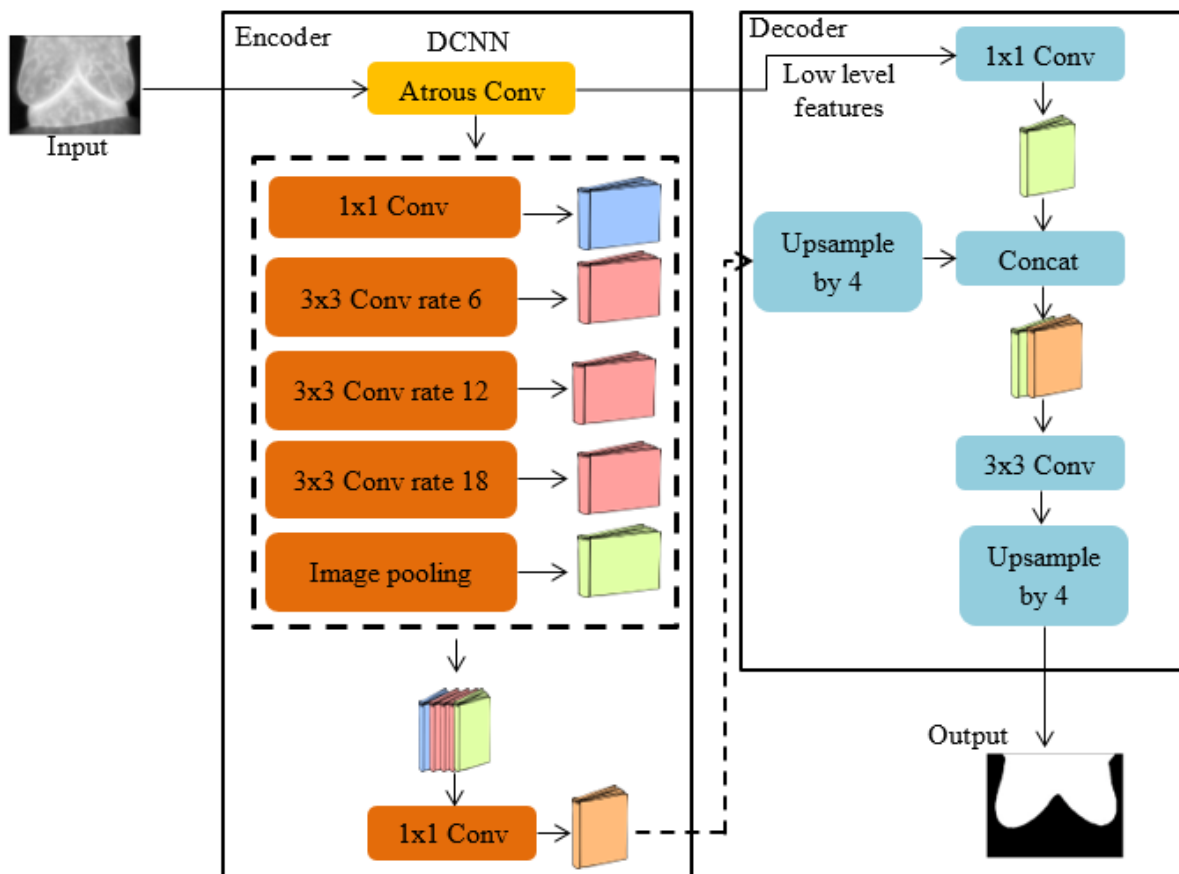


Fig 1: Proposed deep learning framework named ROISegNet for ROI segmentation from breast thermograms

Additionally, we may deliberately regulate the density at which feature responses in fully convolutional networks are computed thanks to atrous convolution. Here, the output stride shows the proportion of the spatial resolution of the input image to the final output resolution. The final feature responses (before fully connected layers or global pooling) for the DCNNs [44], [45] used for the image classification task are 32 times smaller than the input picture dimension, yielding an output stride of 32. In order to avoid signal decimation, the final pooling or convolutional layer's resolution-reducing stride is set to 1 in order to obtain a maximum of 16 output strides (doubling the spatial density of computed feature responses in the DCNNs). Atrous convolutional layers with rate $r = 2$ then replace all ensuing convolutional layers. As a result, we can extract denser feature responses without having to pick up any new skills. Kindly consult [48] for further information.

3.2. Design of Atrous Convolution

Firstly, we investigate the design of atrous convolution modules stacked in a cascade configuration. More precisely, what we do is duplicate the last ResNet block and arrange them in a cascade. These blocks have final convolution and three 3×3 convolutions apart from the one in the final block contains stride 2, much like the original ResNet. This approach is motivated by the fact that long-range information may be easily captured in the

deeper blocks thanks to the striding that has been included. For instance, the final small resolution feature map might provide an overview of the whole picture feature. Consequently, Atrous convolution is carried out at rates that are based on the desired output stride value. Nevertheless, we see that the consecutive striding ruins detail information, which is harmful for semantic segmentation. We test cascading ResNet blocks up to block 7 in this suggested model which has an output stride of 256 in the absence of an atrous convolution. In the suggested model, we use different atrous rates within blocks 4 to 7 due to our inspiration from multi-grid approaches, which use a hierarchy of grids of varying sizes [49], [50]. To be specific, we specify the speeds at which the three convolutional layers operate in blocks 4 through 7 as Multi Grid = (r_1, r_2, r_3) . Unit rate multiplied by corresponding rate yields atrous pace at which the convolutional layer ends. The rates of the three convolutions in block 4 will be, for instance, $2 * (1, 2, 4) = (2, 4, 8)$ with output stride = 16 and multi grid = $(1, 2, 4)$.

3.3. Pyramid Pooling

We re-examine the concept of atrous spatial pyramid pooling (ASPP) introduced in [48], which applies four concurrent feature map featuring atrous convolutions with different atrous rates. The effectiveness of spatial pyramid pooling [51], [52] in reliably and efficiently identifying

areas of an arbitrary scale via resampling characteristics at multiple scales served as the model for ASPP. We incorporate batch normalization into ASPP, which sets us apart from [48]. Multiple scale data is efficiently captured by ASPP with varying atrous rates. As the sample rate increases, we discover that there are less valid filter weights—that is, weights that are not applied to padded zeros, but rather to the valid feature region. As seen in Fig. 4, a 3×3 filter applied to a 65×65 feature map with different atrous rates yields the desired result. As only the center filter weight is functional, the 3×3 filter degenerates to a basic 1×1 filter when the feature map size is close to the rate value in an extreme scenario rather than collecting the entire picture context.

We use image-level features, akin to [53], to get around this issue and provide global context information to the model. To be more precise, after applying batch normalization and global average pooling to the model's final feature map, we bilinearly upsample the image-level features to the appropriate spatial dimension and input them into a 1×1 convolution with 256 filters [54]. Finally, our enhanced ASPP is composed of (a) the image-level features (Fig. 5), and (b) one 1×1 convolution. When the output stride is 16, there is a convolution and three 3×3 convolutions with speeds of 6, 12, and 18. They all have batch normalization and 256 filters. Recall that when output stride equals 8, rates double. After the features from each branch are concatenated, they go through a final 1×1 convolution that yields the final logits, followed by another 1×1 convolution (this time with 256 filters and batch normalization).

3.4 Decoder Design

The final feature map that encoder computes, which includes both image-level and ASPP features, is referred to as the final feature map. $[k \times k, f]$ is the name of the convolution operation that uses kernel $k \times k$ and f filters. In training and assessment, ResNet-101 [55] as a basis. When output stride = 16, the logits are bilinearly upsampled by 16. This simple bilinear upsampling, a naïve decoder design, produces improved performance—1.2% more accurate than training without this crude decoder. To build on this fundamental basis, our proposed architecture (Figure 1) places the encoder output with the decoder module on top. Three regions are examined by the decoder module to consider alternative design options. First, the encoder module's low-level feature map's channels are minimized using a 1×1 convolution. Secondly, a 3×3 convolution is used to provide segmentation results that are more accurate. Thirdly, the choice of low-level encoder characteristics. In particular, utilizing the final feature map in the res2x residual block and the Conv2 features from the ResNet-101 network backbone, we assess the impact of the 1×1 convolution in the decoder module $[3 \times 3, 256]$. Reducing the number

of channels to 48 or 32 in the encoder module's low-level feature map improves performance. Hence, for channel reduction, we choose $[1 \times 1, 48]$.

The 3×3 convolutional architecture for the module decoder is then designed, and the better ROI segmentation is witnessed. We discover that utilizing two 3×3 convolutions with 256 filters is more successful than using just one or three convolutions following the encoding of the encoder feature map with the Conv2 feature map (before to striding). Performance is decreased when one changes the kernel size from 3×3 to 1×1 or the number of filters from 256 to 128. We also test the scenario in which the decoder module uses feature maps from both Conv2 and Conv3. This example involves gradually upsampling two times the decoder feature map, concatenating it with Conv3 first, then Conv2, then refining each using the $[3 \times 3, 256]$ operation. After that, the entire decoding process resembles the U-Net/SegNet architecture [56]. We haven't noticed any appreciable improvement, though. Ultimately, we utilize the extremely basic yet efficient decoder module: two $[3 \times 3, 256]$ operations refine the joining together of the channel-reduced Conv2 the encoder feature map as well as the feature map. Take note that the output stride = 4 of our suggested model. Because of the restricted GPU resources, we have not investigated output feature maps with richer content (i.e., output stride < 4).

3.5 Proposed Algorithm

We proposed an algorithm named Learning based Breast ROI Segmentation (LbBROIS) to realize our framework. Algorithm 1 outlines our algorithm and its modus operandi.

Algorithm: Learning based Breast ROI Segmentation (LbBROIS)

Input: DMR-IR dataset D

Output: Breast ROI segmentation results R, performance statistics P

1. Begin
2. $(T1, T2) \leftarrow \text{DataSplit}(D)$
3. Build ROIsegNet
4. Add encoder network
5. Add decoder network
6. Compile ROIsegNet
7. $LF \leftarrow \text{Get low level features from encoder}(T1)$
8. $F \leftarrow \text{Dense feature extraction by encoder}(T1)$
9. $F' \leftarrow \text{Concatenate}(LF, F)$
10. Train the model
11. $R \leftarrow \text{ROI Segmentation}(F', T2)$
12. $P \leftarrow \text{Evaluation}(R, \text{ground truth masks})$
13. Print R
14. Print P
15. End

Algorithm 1: Learning based Breast ROI Segmentation

Our algorithm LbBROIS takes DMR-IR dataset D as input. It has provision for pre-processing of given dataset by splitting it into training and testing datasets. ROIsegNet is the proposed network which is built and compiled. The encoder is made up of Atrous convolution that has potential to have probing of convolutional features at different scales by employing different rates. It generates both image level dense features and also low level features. The concatenation of both kinds of features leads to final feature map that is employed to educate the model. After training the model, it can be persisted and used for semantic segmentation of breast ROI from thermal images. The model takes test images and the decoder helps in refining results of segmentation along with boundaries of objects. The suggested model's outcomes are contrasted with the ground truth to arrive at performance statistics.

3.6 Evaluation Method

The suggested model is assessed using number of performance metrics that are derived from confusion matrix as illustrated in Figure 2.

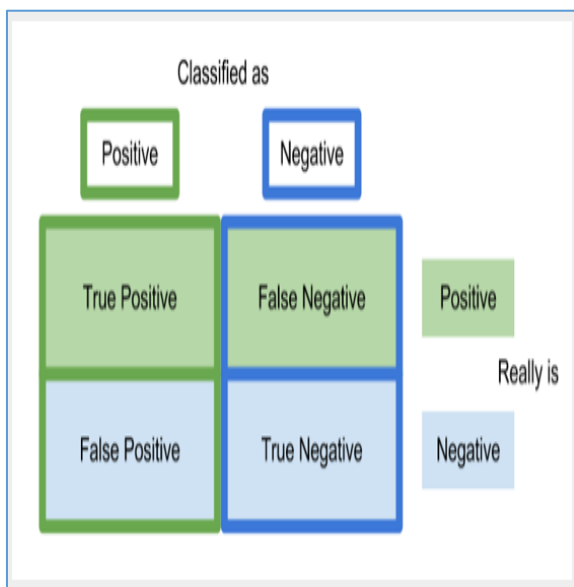


Fig 2: Confusion matrix

Precision is a metric used to compute correctly classified pixels' proportion as positive to all pixels classified as positive. This metric is as expressed in Eq. 2.

$$\text{Precision (p)} = \frac{TP}{TP+FP} \quad (2)$$

Accuracy is another metric used to measure correctly classified proportion of pixels in relation with total pixels in the given image. This metric is as expressed in Eq. 3.

$$\text{Accuracy} = \frac{TP+TN}{TP+TN+FP+FN} \quad (3)$$

Intersection over union metric, on the other hand, is used to find the overlap in the anticipated mask and the ground truth mask. It is computed as in Eq. 4.

$$\text{IoU} = \frac{TP}{(TP+FP+FN)} \quad (4)$$

4. Experimental Results

Our framework ROIsegNet is evaluated with a benchmark dataset known as DMR-IR [41]. It was collected from Hospital of UFF University. In this study we used 1000 breast thermograms comprising of both positive and negative breast cancer samples divided into testing, testing and validation sets. The aim of the proposed framework is to perform ROI segmentation that is useful further in breast cancer screening.

4.1 Results

This section presents results of our empirical study. Figure 3 shows an excerpt from DMR-IR breast thermograms dataset.

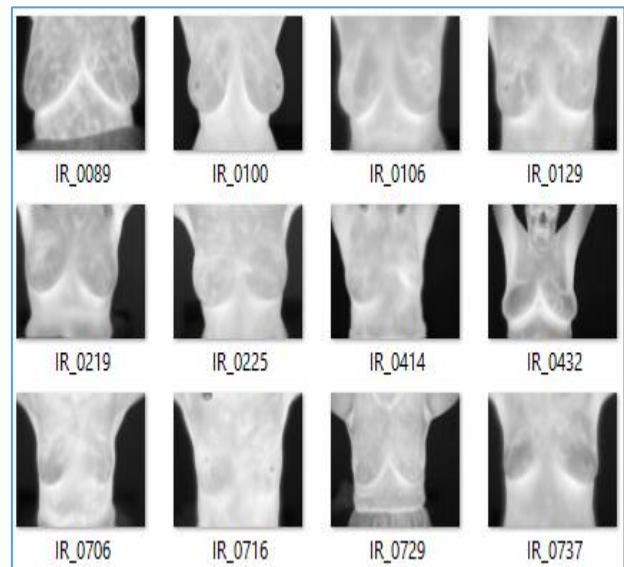


Fig 3: An excerpt from DMR breast thermograms dataset

Data augmentation is used to increase data diversity towards leveraging training quality besides minimizing the overfitting problem. Figure 4 shows a portion of results of data augmentation.

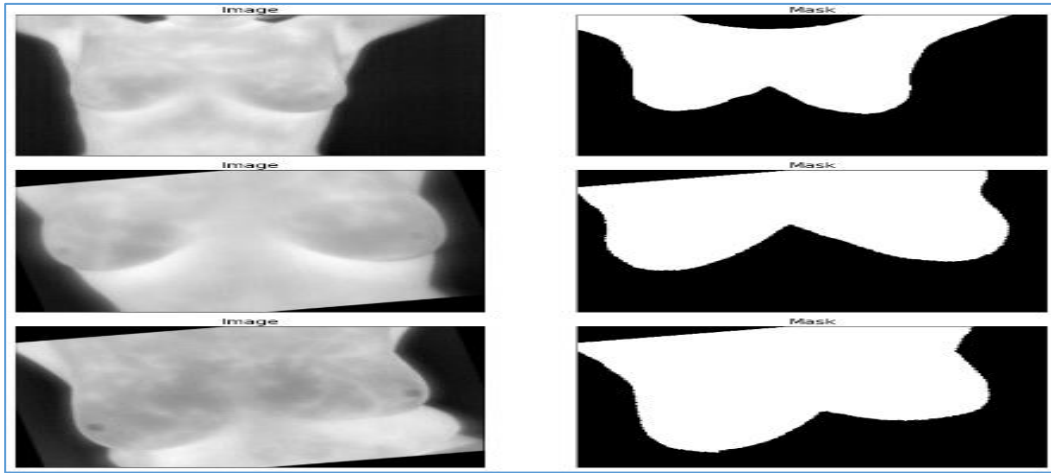
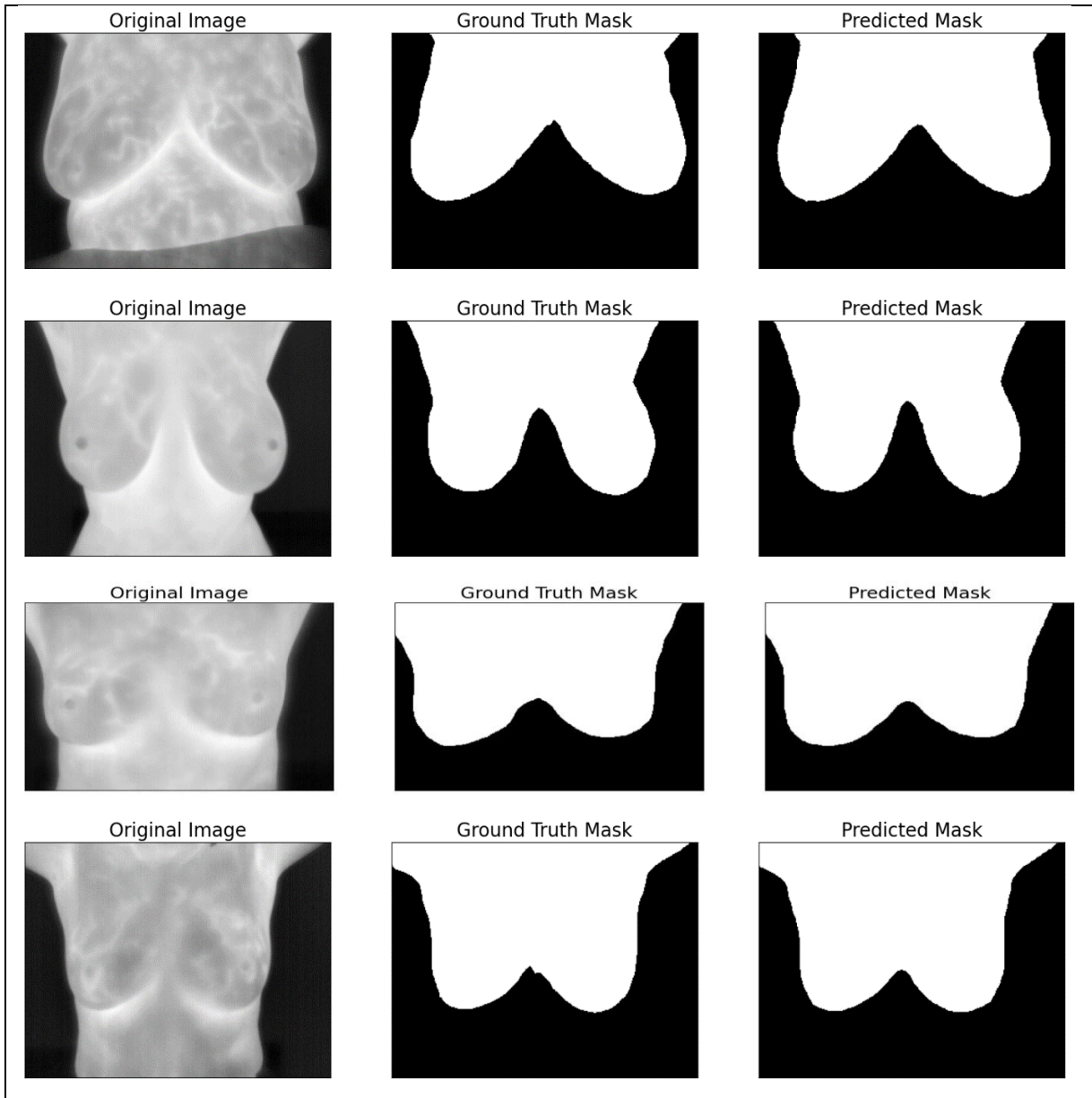


Fig 4: Results of data augmentation

The augmented data is given to put the suggested model through training. The model comprises of encoder and decoder architectures as illustrated in Figure 1. The model is found efficient in finding region of interest and visualizing the same. Figure 5 presents an excerpt from our experimental results in terms of original breast thermogram, ground truth mask and predicted mark.



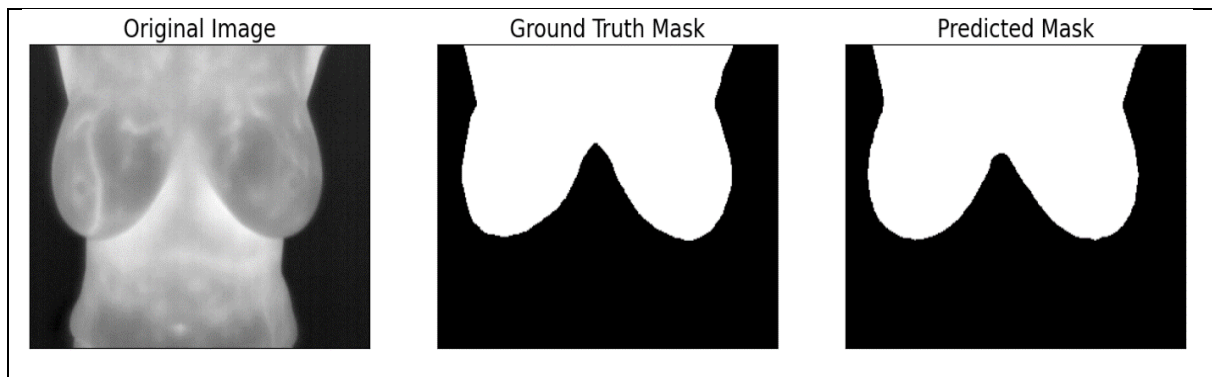


Fig 5: An excerpt from the experimental results reflecting ROI segmentation

ROI segmentation results revealed that the proposed model is able to perform segmentation of breast thermograms correctly. Based on anomalies discovered in the ROI, the resulting segmented pictures may be utilized for breast cancer probability detection and classification. The outcomes of precise segmentation based on ROI are displayed in Figure 6.

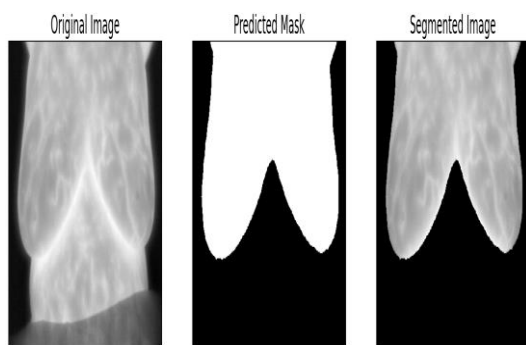


Fig 6: Result of segmentation

Additional evaluations of the suggested model's performance are conducted in terms of dice loss, accuracy, IoU, and precision. The precise performance of the suggested model is displayed in Figure 7.

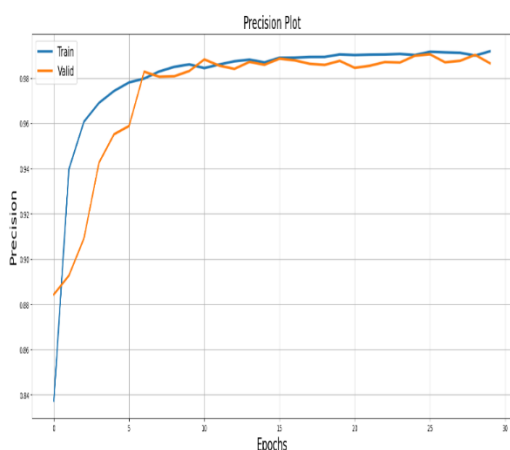


Fig 7: Performance of the proposed model in terms precision

Precision of the model is presented against number of epochs. As the number of epochs is increased, the precision value is gradually increased. By the time, it reaches 30 epochs the model has converged to highest

precision. Figure 8 shows accuracy exhibited by the proposed model.

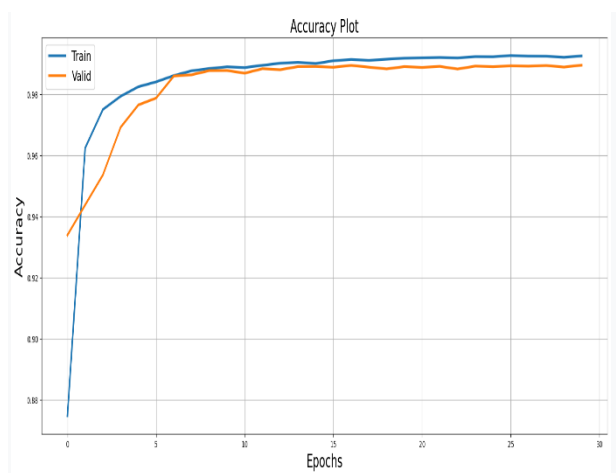


Fig 8: Performance of the proposed model in terms accuracy

The model's accuracy is displayed in relation to the number of epochs. As the number of epochs is increased, the accuracy value is gradually increased. By the time, it reaches 30 epochs the model has converged to highest accuracy. Figure 9 shows IoU score exhibited by the proposed model.

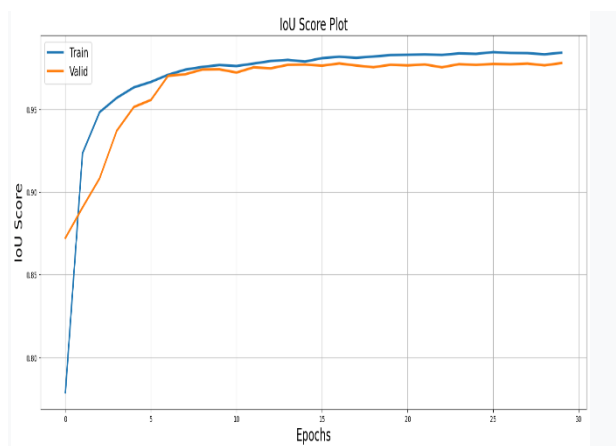


Fig 9: Performance of the proposed model in terms IoU score

IoU of the model is presented against number of epochs. As the number of epochs is increased, the IoU value is gradually increased. By the time, it reaches 30 epochs the

model has converged to highest IoU. Figure 10 shows dice loss performance exhibited by the proposed model.

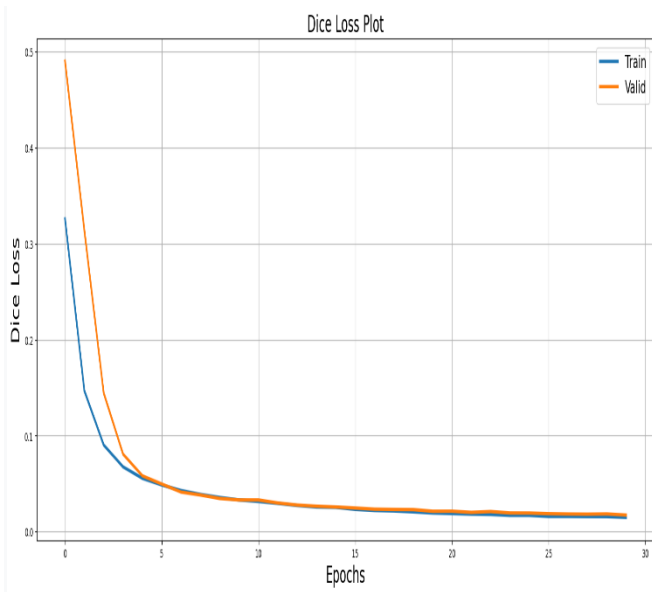


Fig 10: Performance of the proposed model in terms dice loss

Dice loss of the model is presented against number of epochs. Lower in dice loss indicates better performance. As the number of epochs is increased, the dice loss value is gradually decreased. By the time, it reaches 30 epochs the model has converged to least dice loss. Table 1 shows the converged performance exhibited by the proposed model in terms of all evaluation metrics.

Metric	Value
Mean Accuracy	0.9863
Mean IoU Score	0.9706
Mean Precision Score	0.9811
Mean Dice Loss	0.0213

Table 1: Shows performance of the proposed model

Figure 11 displays the performance of the suggested approach using several criteria used to evaluate its capability in ROI segmentation of brain thermograms.

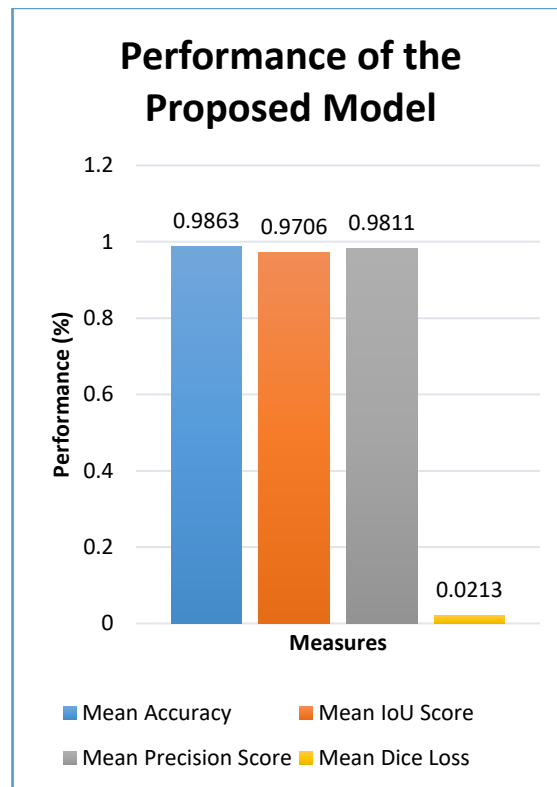


Fig 11: Performance of the proposed model

Mean dice loss of the proposed model is 0.0213 which is lowest at the last epoch in the model execution. Mean precision is 98.11% while the mean IoU score is 97.06%. The mean accuracy of the model is 98.63%.

4.2 Performance Comparison

Our model ROIsegNet is compared with many existing models used for ROI segmentation on breast thermograms. The existing models used for comparison include VGG19 [56], ResNet50 [57], InceptioV3 [58] and Atrous Convolution [55]. Table 2 shows the performance statistics of different models.

Segmentation Model	Performance (%)			
	Mean Precision	Mean IoU Score	Mean Accuracy	Mean Dice Loss
VGG19	90.4935	89.525	90.9731	0.023
ResNet50	92.3403	91.352	92.8297	0.0226
InceptionV3	94.2248	93.2164	94.7242	0.0221
Atrous Convolution	96.1478	95.1188	96.6574	0.0217
ROIsegNet	98.1101	97.0623	98.6312	0.0208

Table 2: Performance comparison

The suggested ROIsegNet model's performance is contrasted with that of many other models currently in use. Figure 12 shows the visualization of mean dice loss comparison.

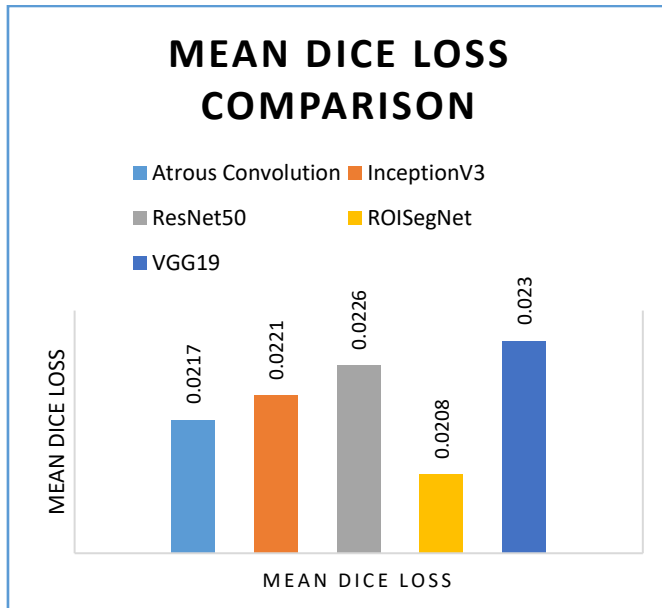


Fig 12: Performance comparison in terms of mean dice loss

Mean dice loss of VGG19 model is 0.023. Mean dice loss of ResNet50 is 0.0226, InceptionV3 0.0221 and Atrous convolution 0.0217. Lowest dice loss is exhibited by the proposed model 0.0208. The suggested model performs better than the current models in terms of mean dice loss, according to the results. The performance comparison of all models is displayed in Figure 13 in terms of mean accuracy, mean IoU score, and mean precision.

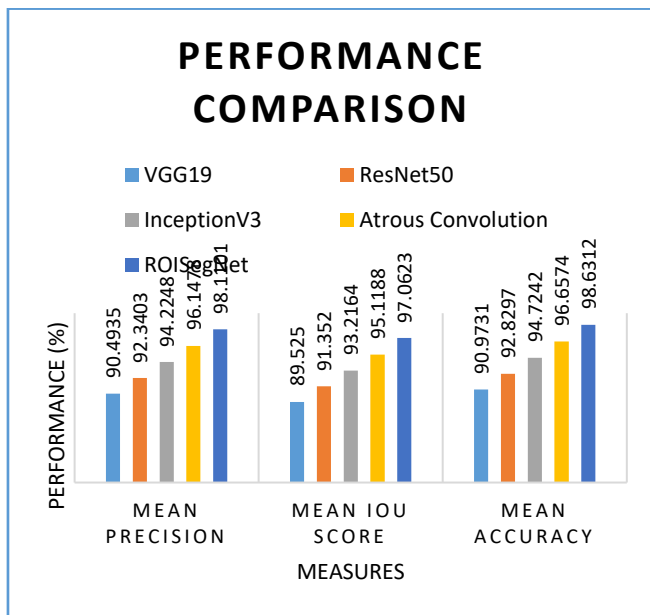


Fig 13: Performance comparison in terms of mean precision, mean IoU score and mean accuracy

Mean precision value of VGG19 is 90.49%, ResNet50 92.34%, InceptionV3 94.22%, Atrous Convolution

96.14% and ROIsegNet exhibited 98.11% as mean precision score. Mean IoU score of VGG19 is 89.52%, ResNet50 91.35%, InceptionV3 93.21%, Atrous Convolution 95.11% and ROIsegNet exhibited 97.06% as mean IoU score. Mean accuracy value of VGG19 is 90.97%, ResNet50 92.82%, InceptionV3 94.72%, Atrous Convolution 96.65% and ROIsegNet exhibited 98.63% as mean accuracy. From the experimental results, it is observed that the proposed model outperformed other existing models in ROI segmentation of breast thermograms. The rationale behind performance improvement of ROIsegNet is that, it has different optimizations including a decoder module designed to extend the model based on Atrous Convolution.

5. Discussion

5.1 Limitations

6. Conclusion and Future Work

We suggested a deep learning architecture called ROIsegNet for automatic segmentation of ROI from breast thermogram imagery. Our framework uses atrous convolution as part of encoder and designs decoder module for leveraging efficiency in semantic segmentation. The framework is based on the design of encoder-decoder made up of atrous convolution as part of encoder and a customized decoder network. The given input breast thermal image is subjected to efficient segmentation to obtain ROI (breast region) which helps in automatic detection of abnormalities that might lead to breast cancer in future. We proposed an algorithm named Learning based Breast ROI Segmentation (LbBROIS) to realize our framework. Our empirical study made with the benchmark dataset DMR-IR revealed with, ROIsegNet outperforms existing models such as VGG19, ResNet50, InceptionV3 and Atrous Convolution with highest accuracy 98.63%. Our framework has a significant limitation as it confines to ROI segmentation and does not focus on breast cancer detection. In our future work, we will develop a novel breast abnormality grading system for identifying asymptomatic patients.

References

- [1] R. Karthiga and K. Narasimhan; (2021). Medical imaging technique using curvelet transform and machine learning for the automated diagnosis of breast cancer from thermal image . Pattern Analysis and Applications. <http://doi:10.1007/s10044-021-00963-3>
- [2] Samir S. Yadav and Shivajirao M. Jadhav. (2020). Thermal infrared imaging based breast cancer diagnosis using machine learning techniques. *Springer*. 81, pp.1-19. <https://doi.org/10.1007/s11042-020-09600-3>

- [3] Raquel Sánchez-Cauce; Jorge Pérez-Martín and Manuel Luque; (2021). Multi-input convolutional neural network for breast cancer detection using thermal images and clinical data . *Computer Methods and Programs in Biomedicine*. <http://doi:10.1016/j.cmpb.2021.106045>
- [4] Mariana Macedo; Maira Santana; Wellington P. dos Santos; Ronaldo Menezes and Carmelo Bastos-Filho; (2021). Breast cancer diagnosis using thermal image analysis: A data-driven approach based on swarm intelligence and supervised learning for optimized feature selection . *Applied Soft Computing*. <http://doi:10.1016/j.asoc.2021.107533>
- [5] Barsha Abhisheka, Saroj Kumar Biswas and Biswajit Purkayastha. (2023). A comprehensive review on breast cancer detection, classification and segmentation using deep learning. *Springer*. 30, pp.1-30. <https://doi.org/10.1007/s11831-023-09968-z>
- [6] DENNIES TSIETSO, ABID YAHYA, RAVI SAMIKANNU, MUHAMMAD USMAN TARIQ, MUHAMMAD BABAR, BASIT QURESHI AND ANIS KOUBAA. (2023). Multi-Input Deep Learning Approach for Breast Cancer Screening Using Thermal Infrared Imaging and Clinical Data. *IEEE*. 11, pp.52101 - 52116. <http://DOI:10.1109/ACCESS.2023.3280422>
- [7] Venkatesan Rajinikanth; Seifedine Kadry; David Taniar; Robertas Damasevicius and Hafiz Tayyab Rauf; (2021). Breast-Cancer Detection using Thermal Images with Marine-Predators-Algorithm Selected Features . 2021 Seventh International conference on Bio Signals, Images, and Instrumentation (ICBSII). <http://doi:10.1109/icbsii51839.2021.9445166>
- [8] Houssein, Essam H.; Emam, Marwa M.; Ali, Abdelmgeid A. and Suganthan, Ponnuthurai Nagaratnam (2020). Deep and machine learning techniques for medical imaging-based breast cancer: A comprehensive review. *Expert Systems with Applications*, 114161–. <http://doi:10.1016/j.eswa.2020.114161>
- [9] Aigerim Mashekova, Yong Zhao, Eddie Y.K. Ng, Vasilios Zarikas, Sai Cheong Fok and Olzhas Mukhmetov. (2022). Early detection of the breast cancer using infrared technology – A comprehensive review. *Elsevier*. 27, pp.1-18. <https://doi.org/10.1016/j.tsep.2021.101142>
- [10] Resmini, R., Faria da Silva, L., Medeiros, P. R. T., Araujo, A. S., Muchaluat-Saade, D. C., & Conci, A. (2021). A hybrid methodology for breast screening and cancer diagnosis using thermography. *Computers in Biology and Medicine*, 135, 104553. <http://doi:10.1016/j.compbiomed.2021.104553>
- [11] Houssein, E. H., Emam, M. M., & Ali, A. A. (2021). An efficient multilevel thresholding segmentation method for thermography breast cancer imaging based on improved chimp optimization algorithm. *Expert Systems with Applications*, 185, 115651. <http://doi:10.1016/j.eswa.2021.115651>
- [12] Lakshman K; Siddharth B. Dabhade; Y. S. Rode; Karan Dabhade; S. Deshmukh and Ranjan Maheshwari; (2021). Identification of Breast Cancer from Thermal Imaging using SVM and Random Forest Method . 2021 5th International Conference on Trends in Electronics and Informatics (ICOEI). <http://doi:10.1109/icoei51242.2021.9452809>
- [13] Zeiser, F. A., da Costa, C. A., Ramos, G. de O., Bohn, H. C., Santos, I., & Roehe, A. V. (2021). *DeepBatch: A hybrid deep learning model for interpretable diagnosis of breast cancer in whole-slide images*. *Expert Systems with Applications*, 185, 115586. <http://doi:10.1016/j.eswa.2021.115586>
- [14] Zahra Rezaei; (2021). A review on image-based approaches for breast cancer detection, segmentation, and classification . *Expert Systems with Applications*. <http://doi:10.1016/j.eswa.2021.115204>
- [15] Liu, Z., Ni, S., Yang, C., Sun, W., Huang, D., Su, H., ... Qin, N. (2021). Axillary lymph node metastasis prediction by contrast-enhanced computed tomography images for breast cancer patients based on deep learning. *Computers in Biology and Medicine*, 136, 104715. <http://doi:10.1016/j.compbiomed.2021.104715>
- [16] Krithiga, R. and Geetha, P. (2020). Breast Cancer Detection, Segmentation and Classification on Histopathology Images Analysis: A Systematic Review. *Archives of Computational Methods in Engineering*. <http://doi:10.1007/s11831-020-09470-w>
- [17] Sharma, R., Sharma, J. B., Maheshwari, R., & Baleanu, D. (2021). Early anomaly prediction in breast thermogram by hybrid model consisting of superpixel segmentation, sparse feature descriptors and extreme learning machine classifier. *Biomedical Signal Processing and Control*, 70, 103011. <http://doi:10.1016/j.bspc.2021.103011>
- [18] Jun Bai; Russell Posner; Tianyu Wang; Clifford Yang and Sheida Nabavi; (2021). Applying deep learning in digital breast tomosynthesis for automatic breast cancer detection: A review . *Medical Image Analysis*. <http://doi:10.1016/j.media.2021.102049>
- [19] Bardia Yousefi; Hossein Memarzadeh Sharifipour and Xavier P. V. Maldague; (2021). A Diagnostic Biomarker for Breast Cancer Screening via Hilbert Embedded Deep Low-Rank Matrix Approximation .

- IEEE Transactions on Instrumentation and Measurement.
<http://doi:10.1109/tim.2021.3085956>
- [20] Chen Chen; Yong Wang; Jianwei Niu; Xuefeng Liu; Qingfeng Li and Xuandong Gong; (2021). Domain Knowledge Powered Deep Learning for Breast Cancer Diagnosis Based on Contrast-Enhanced Ultrasound Videos . IEEE Transactions on Medical Imaging. <http://doi:10.1109/tmi.2021.3078370>
- [21] Tariq, Mehreen; Iqbal, Sajid; Ayesha, Hareem; Abbas, Ishaq; Ahmad, Khawaja Tehseen and Niazi, Muhammad Farooq Khan (2020). Medical Image based Breast Cancer Diagnosis: State of the Art and Future Directions. Expert Systems with Applications, 114095–. <http://doi:10.1016/j.eswa.2020.114095>
- [22] Nienke Bakx, Dorien Rijkaart, Maurice van der Sangen, Jacqueline Theuws , Peter-Paul van der Toorn, An-Sofie Verrijssen, Jorien van der Leer, Joline Mutsaers, Th'er`ese van Nunen, Marjon Reinders, Inge Schuengel, Julia Smits, Els Hagelaar, Dave van Gruijthuisen, Johanna Bluemink and Coen Hurkmans. (2023). Clinical evaluation of a deep learning segmentation model including manual adjustments afterwards for locally advanced breast cancer. *Elsevier*. 26, pp.1-6. <https://doi.org/10.1016/j.tipsro.2023.100211>
- [23] Rahul Kumar Yadav, Pardeep Singh and Poonam Kashtriya. (2023). Diagnosis of Breast Cancer using Machine Learning Techniques -A Survey. *Elsevier*. 218, pp.1434-1443. <https://doi.org/10.1016/j.procs.2023.01.122>
- [24] Chang Li and Xi Lu; (2021). Computer-Aided Detection Breast Cancer in Whole Slide Image . 2021 International Conference on Computer, Control and Robotics (ICCCR). <http://doi:10.1109/icccr49711.2021.9349391>
- [25] Seifedine Kadry; Robertas Damasevicius; David Taniar; Venkatesan Rajinikanth and Isah A. Lawal; (2021). Extraction of Tumour in Breast MRI using Joint Thresholding and Segmentation – A Study . 2021 Seventh International conference on Bio Signals, Images, and Instrumentation (ICBSII). <http://doi:10.1109/icbsii51839.2021.9445152>
- [26] Yun Peng, Wei Tang and Xiaoyu Peng. (2023). The study of ultrasonography based on deep learning in breast cancer. *Elsevier*. 16(4), pp.1-7. <https://doi.org/10.1016/j.jrras.2023.100679>
- [27] Sruthi Krishna and Betsy George; (2021). An affordable solution for the recognition of abnormality in breast thermogram . Multimedia Tools and Applications. <http://doi:10.1007/s11042-021-11082-w>
- [28] Jessiane M. S. Pereira; Maíra A. Santana; Juliana C. Gomes; Valter Augusto de Freitas Barbosa; Mêuser Jorge Silva Valença; Sidney Marlon Lopes de Lima and Wellington Pinheiro dos Santos; (2021). Feature selection based on dialectics to support breast cancer diagnosis using thermographic images . Research on Biomedical Engineering. <http://doi:10.1007/s42600-021-00158-z>
- [29] Meenalochini, G. and Ramkumar, S. (2020). Survey of machine learning algorithms for breast cancer detection using mammogram images. Materials Today: Proceedings, S2214785320364257–. <http://doi:10.1016/j.matpr.2020.08.543>
- [30] Mishra, S., Prakash, A., Roy, S. K., Sharan, P., & Mathur, N. (2020). Breast Cancer Detection using Thermal Images and Deep Learning. 2020 7th International Conference on Computing for Sustainable Global Development (INDIACom). doi:10.23919/indiacom49435.2020.9083722
- [31] Ibrahim, Abdelhameed; Mohammed, Shaimaa; Ali, Hesham Arafat and Hussein, Sherif E. (2020). Breast Cancer Segmentation from Thermal Images Based on Chaotic Salp Swarm Algorithm. IEEE Access, 1–1. <http://doi:10.1109/ACCESS.2020.3007336>
- [32] Kakileti, Siva Teja; Manjunath, Geetha and Madhu, Himanshu J. (2019). 41st Annual International Conference of the IEEE Engineering in Medicine and Biology Society (EMBC) - Cascaded CNN for View Independent Breast Segmentation in Thermal Images. 6294–6297. <http://doi:10.1109/embc.2019.8856628>
- [33] Husaini, Mohammed Abdulla Salim Al; Habaebi, Mohamed Hadi; Hameed, Shihab A.; Islam, Md. Rafiqul and Gunawan, Teddy Surya (2020). A Systematic Review of Breast Cancer Detection Using Thermography and Neural Networks. IEEE Access, 8, 208922–208937. <http://doi:10.1109/ACCESS.2020.3038817>
- [34] Raghavendra, U; Gudigar, Anjan; Rao, Tejaswi N; Ciaccio, Edward J; Ng, E.Y.K. and Rajendra Acharya, U. (2019). Computer aided diagnosis for the identification of breast cancer using thermogram images: A comprehensive review. Infrared Physics & Technology, 103041–. <http://doi:10.1016/j.infrared.2019.103041>
- [35] Farooq, Muhammad Ali and Corcoran, Peter (2020). 31st Irish Signals and Systems Conference (ISSC) - Infrared Imaging for Human Thermography and Breast Tumor Classification using Thermal Images. 1–6. <http://doi:10.1109/ISSC49989.2020.9180164>
- [36] Singh, Deepika and Singh, Ashutosh Kumar (2020). Role of image thermography in early breast cancer detection- Past, present and future. Computer Methods and Programs in Biomedicine, 183,

105074–.

<http://doi:10.1016/j.cmpb.2019.105074>

- [37] Kakileti, Siva Teja; Madhu, Himanshu J.; Manjunath, Geetha; Wee, Leonard; Dekker, Andre and Sampangi, Sudhakar (2020). Personalized risk prediction for breast cancer pre-screening using artificial intelligence and thermal radiomics. *Artificial Intelligence in Medicine*, 105, 101854–. <http://doi:10.1016/j.artmed.2020.101854>
- [38] Sánchez-Ruiz, Daniel; Olmos-Pineda, Ivan and Olvera-López, J. Arturo (2020). Automatic region of interest segmentation for breast thermogram image classification. *Pattern Recognition Letters*, 135, 72–81. <http://doi:10.1016/j.patrec.2020.03.025>
- [39] Mahmood, Tariq; Li, Jianqiang; Pei, Yan; Akhtar, Faheem; Imran, Azhar and Rehman, Khalil ur (2020). A Brief Survey on Breast Cancer Diagnostic with Deep Learning Schemes Using Multi-Image Modalities. *IEEE Access*, 1–1. <http://doi:10.1109/ACCESS.2020.3021343>
- [40] P, Gomathi; C, Muniraj and PS, Periasamy (2020). BREAST THERMOGRAPHY BASED UNSUPERVISED ANISOTROPIC- FEATURE TRANSFORMATION METHOD FOR AUTOMATIC BREAST CANCER DETECTION. *Microprocessors and Microsystems*, 103137–. <http://doi:10.1016/j.micpro.2020.103137>
- [41] DMR - Database for Mastology Research. Retrieved from <http://visual.ic.uff.br/dmi/>
- [42] Y. LeCun, B. Boser, J. S. Denker, D. Henderson, R. E. Howard, W. Hubbard, and L. D. Jackel. Backpropagation applied to handwritten zip code recognition. *Neural computation*, 1(4):541–551, 1989.
- [43] P. Sermanet, D. Eigen, X. Zhang, M. Mathieu, R. Fergus, and Y. LeCun. Overfeat: Integrated recognition, localization and detection using convolutional networks. arXiv:1312.6229, 2013.
- [44] Krizhevsky, I. Sutskever, and G. E. Hinton. Imagenet classification with deep convolutional neural networks. In NIPS, 2012.
- [45] K. Simonyan and A. Zisserman. Very deep convolutional networks for large-scale image recognition. In ICLR, 2015.
- [46] M. Holschneider, R. Kronland-Martinet, J. Morlet, and P. Tchamitchian. A real-time algorithm for signal analysis with the help of the wavelet transform. In *Wavelets: Time-Frequency Methods and Phase Space*, pages 289–297. 1989.
- [47] Giusti, D. Ciresan, J. Masci, L. Gambardella, and J. Schmidhuber. Fast image scanning with deep max-pooling convolutional neural networks. In ICIP, 2013.
- [48] L.- C.Chen,G.Papandreou,I.Kokkinos,K.Murphy,andA. L. Yuille. Deeplab: Semantic image segmentation with deep convolutional nets, atrous convolution, and fully connected crfs. arXiv:1606.00915, 2016.
- [49] Brandt. Multi-level adaptive solutions to boundary-value problems. *Mathematics of computation*, 31(138):333–390, 1977.
- [50] D. Terzopoulos. Image analysis using multigrid relaxation methods. *TPAMI*, (2):129–139, 1986.
- [51] K. Grauman and T. Darrell. The pyramid match kernel: Discriminative classification with set of image features . In ICCV, 2005.
- [52] S. Lazebnik, C. Schmid, and J. Ponce. Beyond bags of features: Spatial pyramid matching for recognizing natural scene categories. In CVPR, 2006.
- [53] W. Liu, A. Rabinovich, and A. C. Berg. Parsenet: Looking wider to see better. arXiv:1506.04579, 2015.
- [54] S. Ioffe and C. Szegedy. Batch normalization: Accelerating deep network training by reducing internal covariate shift. arXiv:1502.03167, 2015.
- [55] Chen, L.C., Papandreou, G., Schroff, F., Adam, H.: Rethinking atrous convolution for semantic image segmentation. arXiv:1706.05587 (2017)
- [56] Ronneberger, O., Fischer, P., Brox, T.: U-net: Convolutional networks for biomedical image segmentation. In: MICCAI. (2015).
- [56] Sandeep Wadekar, Dileep Kumar Singh. (2023). A modified convolutional neural network framework for categorizing lung cell histopathological image based on residual n. Elsevier. 4, pp.1-8. [Online]. Available at: <https://doi.org/10.1016/j.health.2023.100224>
- [57] MYASAR MUNDHER ADNAN, MOHD SHAFRY MOHD RAHIM, AMJAD REHMAN KHAN. (2023). Automated Image Annotation with Novel Features Based on Deep ResNet50-SLT. *IEEE*. 11, pp.40258-40277. [Online]. Available at: Digital Object Identifier 10.1109/ACCESS.2023.3266296.
- [58] Liu, Zhiyong; Yang, Chuan; Huang, Jun; Liu, Shaopeng; Zhuo, Yumin; Lu, Xu (2021). Deep learning framework based on integration of S-Mask R-CNN and Inception-v3 for ultrasound image-aided diagnosis of prostate cancer. *Future Generation Computer Systems*, 114, pp.358–367. doi:10.1016/j.future.2020.08.015